

# Generalized Gross–Neveu Models and Chiral Symmetry Breaking from String Theory

Anirban Basu<sup>*a*1</sup> and Anshuman Maharana<sup>*b*2</sup>

<sup>*a*</sup> Institute for Advanced Study, Princeton, NJ 08540, USA

<sup>*b*</sup> Department of Physics, University of California Santa Barbara,  
Santa Barbara, CA 93106, USA

## Abstract

We consider intersecting D-brane models which have two dimensional chiral fermions localized at the intersections. At weak coupling, the interactions of these fermions are described by generalized Gross–Neveu models. At strong coupling, these configurations are described by the dynamics of probe D-branes in a curved background spacetime. We study patterns of dynamical chiral symmetry breaking in these models at weak and strong coupling, and also discuss relationships between these two descriptions.

---

<sup>1</sup>email: abasu@ias.edu

<sup>2</sup>email: anshuman@physics.ucsb.edu

# 1 Introduction

Four dimensional Quantum Chromodynamics (QCD) describes the force of strong interactions in nature. This theory is asymptotically free and is strongly coupled at low energies, thus making it difficult to analyze. In particular, it has proven difficult to solve the theory even in the limit of large number of colors. In the limit in which the quark masses in the QCD Lagrangian can be neglected, this theory has a chiral flavor symmetry which is broken in the presence of the mass terms. Understanding the dynamics of chiral symmetry breaking in strongly coupled gauge theories continues to be a challenge.

An extremely successful phenomenological model to understand chiral symmetry breaking in  $\text{QCD}_4$  was developed originally by Nambu and Jona-Lasinio (NJL) [1] where they constructed a field theory of chiral fermions with a four-fermion interaction. In this model, the chiral flavor symmetry gets dynamically broken to the diagonal subgroup and the mesons are identified with the Nambu-Goldstone bosons of the broken symmetry generators. However, this four-fermion interaction is non-renormalizable and so the predictions depend on the UV cutoff of the theory.

In two dimensions, an asymptotically free quantum field theory was constructed by Gross and Neveu (GN) [2] which has a renormalizable four-fermion interaction. So the coupling undergoes dimensional transmutation [3], leaving the number of colors as the only free parameter in the theory. This model can be exactly solved in the limit of large number of colors and exhibits dynamical chiral symmetry breaking. Thus the GN model has proven to be an extremely interesting toy model in understanding chiral symmetry breaking in QCD. It should be noted that the chiral symmetry is broken only when the number of colors  $N_c$  is strictly infinite, and is restored for any finite value of  $N_c$  [4, 5], however large. As described in [4], the  $1/N_c$  expansion is reliable in studying the spectrum of this model as well as related ones like the Thirring model. So though we shall continue to use the term “symmetry breaking” as used in the literature, it is important to remember that the fermions are massive, no continuous symmetries are broken, and the massless bosons are not Nambu-Goldstone bosons.

It is believed that string theory techniques will play an important role in understanding strong coupling issues like confinement and chiral symmetry breaking in QCD. A confining pure Yang-Mills  $U(N_c)$  gauge theory in four dimensions was constructed in [6] by compactifying one of the world-volume dimensions of  $N_c$  D4-branes on a circle of radius  $R$  with supersymmetry breaking boundary conditions. The fermions and the scalars of the world volume theory of the D4-branes get masses at tree level and one-loop level respectively, and

so the infra-red theory is pure Yang–Mills which exhibits confinement. In order to model more realistic theories involving chiral fermions, the authors of [7, 8] considered a D–brane configuration involving “flavor” D8-branes alongwith the “color” D4-branes, where the flavor branes intersect the color branes along three spatial dimensions, such that there are no directions transverse to both the flavor and the color branes. The flavor branes are separated by a distance  $L$  along the D4 world–volume. One gets chiral fermions in this model which are given by the 4–8 strings stretching between the flavor and color branes. These chiral fermions are localized at the intersections of the color and flavor branes. Though classically this configuration preserves the chiral flavor symmetry, this model exhibits dynamical chiral symmetry breaking (which is a global symmetry from the point of view of the color brane theory). This was demonstrated at large values of a classically dimensionless coupling constant  $\lambda/L$  (where  $\lambda$  is essentially the ’t Hooft coupling of five dimensional Yang–Mills theory ) in [7], by considering the D8-branes as probes [9]<sup>3</sup> in the near–horizon geometry of the  $N_c$  D4-branes. Chiral symmetry breaking manifests itself as a wormhole solution of the D8-brane action connecting the D8– $\overline{\text{D}8}$  pair.

Now in these models when one takes the transverse separation  $L$  to be of the same order of magnitude as the circle radius  $R$ , the scales of chiral symmetry breaking and confinement are comparable and it becomes harder to analyze the dynamics of chiral symmetry breaking without taking into account the effects of confinement, and vice versa. Thus to look at the dynamics when chiral symmetry is broken but the theory is not confining, one can consider the limit when  $R \rightarrow \infty$ . This has been done in [13]<sup>4</sup> and the configuration has been analyzed in the limits  $\lambda/L \rightarrow 0$  and  $\lambda/L \rightarrow \infty$ , and it has been found that the chiral symmetry is broken in both the regimes. The  $\lambda/L \rightarrow 0$  regime is described by a non–local version of the NJL model (see [15] for a review of phenomenological applications of the non–local NJL model), while the opposite regime is described by a wormhole configuration similar to that mentioned above. It has also been conjectured that these solutions lie in the same universality class as  $\text{QCD}_4$  which is obtained by taking  $R$  to be finite.

A similar analysis to study chiral symmetry breaking in two dimensions has been done in [16]. The D-brane configuration is given by the color D4-branes which intersect the flavor D6-branes along one spatial dimension such that there are no directions transverse to both the color and the flavor branes. Dynamical breaking of chiral symmetry occurs both in the  $\lambda/L \rightarrow 0$  and  $\lambda/L \rightarrow \infty$  limits. The  $\lambda/L \rightarrow 0$  regime is described by the GN model, while the opposite regime is described by a wormhole configuration. This setup is expected

---

<sup>3</sup>Also see [10–12] for related discussions.

<sup>4</sup>The issue of separation of scales was discussed in a different context in [14].

to be in the same universality class as  $\text{QCD}_2$ , which is obtained by wrapping three of the world-volume directions of the D4-branes on  $T^3$ .

In this paper, we generalize the construction of [16] by considering multiple stacks of “flavor” D6 (and  $\overline{\text{D}6}$ )-branes which intersect the “color” D4-branes along one spatial direction. The flavor branes are placed at various points in  $\mathbb{R}^3$  which parametrizes the world-volume directions of the D4-branes that are transverse to the intersection. Our motivation is two-fold: to understand the pattern of chiral symmetry breaking in multi-brane constructions, and to study the relationship between the weak and strong coupling descriptions. In the limit  $\lambda/L_i \rightarrow 0$  (where  $L_i$  refers to the distances between the various D6 and  $\overline{\text{D}6}$  pairs in  $\mathbb{R}^3$ ) the D-brane configurations reduce to generalized GN models<sup>5</sup>, where we exhibit various patterns of chiral symmetry breaking. In the opposite regime, we describe these configurations in terms of probe D6-branes in the near-horizon geometry of the color branes. We find a close relationship between the two descriptions.

The plan of the paper is as follows. We begin by describing the D-brane setup in the next section, followed by the analysis of various setups where all the flavor branes are collinear in the transverse  $\mathbb{R}^3$ . These configurations have some interesting features, and we discuss the relationship between chiral symmetry breaking in the strong and weak coupling limits. We next generalize this construction to flavor branes spanning an  $\mathbb{R}^2$  in  $\mathbb{R}^3$ , and we finally consider general flavor brane configurations in  $\mathbb{R}^3$ .

The pattern of chiral symmetry breaking has distinct features. In all our examples we find that at weak coupling, not all the possible condensates are non-vanishing. The strong coupling analogue of condensates is the presence of wormholes connecting the brane and anti-brane pairs. Just like at weak coupling, the wormhole configuration is also determined by the energetics, and leads to patterns of chiral symmetry breaking similar to weak coupling.

Finally we describe patterns of restoration of the chiral symmetries as the temperature of the system is raised. At a sufficiently high temperature, all the symmetries are restored.

## 2 The D-brane setup

The GN model can be realized in string theory [16] by considering  $N_c$  “color” D4-branes extending along the (01234) directions and two stacks of “flavor” D6 and  $\overline{\text{D}6}$ -branes which extend in the directions (0156789). To discuss generalizations of the GN model, we shall

---

<sup>5</sup>GN models with more than one coupling have been considered, for example, in [17].

consider multiple stacks of D6 and  $\overline{\text{D}6}$ -branes given by

	0	1	2	3	4	5	6	7	8	9
D4	:	x	x	x	x					
D6s, $\overline{\text{D}6}$ s	:	x	x			x	x	x	x	x

All the flavor branes extend in the (0156789) directions, and are located at different points in  $\mathbb{R}^3$  spanned by the directions (234). We shall take every stack of flavor branes to be composed of  $N_f$  branes, our results can be easily generalized to the case where the stacks consist of different numbers of branes.

It is straightforward to deduce the massless spectrum corresponding to these D-brane configurations. Apart from the obvious  $U(N_c)$  gauge theory on the D4-brane world-volume, and the  $U(N_f)_i$  gauge theory on the world-volume of the  $i$ -th stack of  $N_f$  D6 (or  $\overline{\text{D}6}$ )-branes, there are extra normalizable massless modes coming from the 4-6 strings that stretch between the D6 ( $\overline{\text{D}6}$ )-branes and the D4-branes. These massless modes are spacetime fermions coming from the Ramond sector, the lowest modes in the Neveu–Schwarz sector are massive. These 4-6 strings are localized in the directions (01) and give rise to chiral fermions in two dimensions. Thus every stack of D6-branes gives rise to left-moving fermions  $q_L$  which transform in the  $(N_f, N_c)$  of  $U(N_f)_L \times U(N_c)$ . Similarly, every stack of  $N_f$   $\overline{\text{D}6}$ -branes produces right-moving fermions  $q_R$  which transform in the  $(N_f, N_c)$  of  $U(N_f)_R \times U(N_c)$ . Thus the spectrum of a configuration consisting of  $m$  stacks of D6 and  $n$  stacks of  $\overline{\text{D}6}$ -branes has  $m$  left-movers  $q_L$  and  $n$  right-movers  $q_R$ . There is a  $U(N_f)$  symmetry associated with each stack of flavor branes. The fermions are charged under the flavor group of the stack they are localized on, and transform trivially under the flavor group of other stacks.

We will be always working in the limit where  $\alpha' \rightarrow 0$ ,  $g_s \rightarrow 0$ ,  $N_c \rightarrow \infty$ , with  $g_s N_c$  and  $N_f$  fixed<sup>6</sup>. In this limit, the gauge coupling of the flavor branes vanish compared to that of the color branes, so the only relevant coupling is the 't Hooft coupling

$$\lambda = \frac{g_5^2 N_c}{4\pi^2}, \quad (1)$$

where  $g_5^2 = 4\pi^2 g_s \alpha'^{1/2}$  is the dimensionful coupling of the five dimensional Yang–Mills theory. As in [16], we shall discuss the physics of the system in two tractable regimes given

---

<sup>6</sup>Thus, we will not be considering processes involving the annihilation of the branes and the anti-branes.

by the classically dimensionless couplings  $\lambda/L_i \rightarrow 0$  and  $\lambda/L_i \rightarrow \infty$ , where  $L_i$  are the distances between the D6- $\overline{\text{D}6}$  pairs.

In the former limit, the system is well described by an interacting theory of the chiral fermions with the D4-brane gauge field. These fermions are derivatively coupled to the D4-brane scalars and so these couplings vanish in the  $\alpha' \rightarrow 0$  limit. As we shall demonstrate below, one can integrate out the gauge field along the lines of [16] to obtain generalized GN models. The symmetries associated with the flavor stacks  $U(N_f)_L$  for the left-moving fermions, and  $U(N_f)_R$  for the right-moving ones appear as global symmetries.

In the later limit  $\lambda/L_i \rightarrow \infty$ , the 't Hooft coupling  $\lambda$  is large and/or the flavor branes are close to each other. Then the five-dimensional gauge theory effects are large, and we cannot use the above description. However we now have an alternate weakly coupled description [18] which involves analyzing the D6-brane dynamics in the near-horizon geometry of the color D4-branes, which we will also discuss below.

### 3 Three collinear flavor branes

We begin with simplest non-trivial examples of chiral symmetry breaking which involve three stacks of flavor branes placed along a straight line in the  $\mathbb{R}^3$  spanned by the directions (234). These will illustrate the general features of symmetry breaking and vacuum structure in our models. We shall rely heavily on these configurations while discussing later the general flavor brane setups in  $\mathbb{R}^3$ . With three collinear branes, there are two physically distinct orderings<sup>7</sup>, given by  $\overline{\text{D}6} - \text{D}6 - \overline{\text{D}6}$  and  $\text{D}6 - \overline{\text{D}6} - \overline{\text{D}6}$  which we discuss below. In what follows, it will be useful to introduce indices on the stacks of flavor branes. We label the D6-brane stack by 1 and the  $\overline{\text{D}6}$ -brane stacks by labels  $\bar{1}$  and  $\bar{2}$ .

#### 3.1 $\overline{\text{D}6} - \text{D}6 - \overline{\text{D}6}$

Consider a stack of D6-branes and two stacks of  $\overline{\text{D}6}$ -branes placed along the 4 direction in the order  $\overline{\text{D}6} - \text{D}6 - \overline{\text{D}6}$  as shown in figure (1). The stack of D6-branes is located at the origin while the  $\overline{\text{D}6}$ -brane stacks have coordinates  $L_1$  and  $-L_2$  in the 4 direction.

In the regime where the separation between the stack of D6-branes and the stacks of  $\overline{\text{D}6}$ -branes is much larger compared to the five dimensional 't Hooft coupling  $\lambda$ , the effective

---

<sup>7</sup>Other configurations are related to the ones we discuss by charge conjugation.

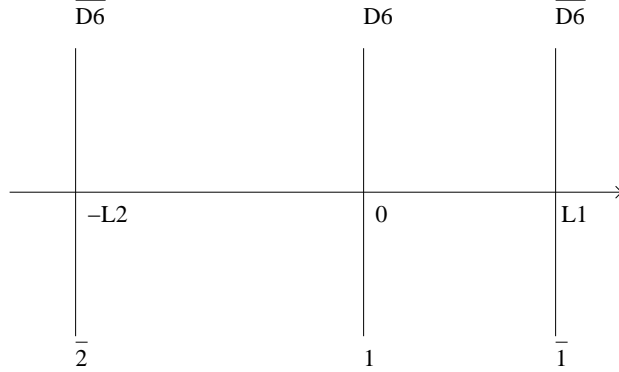


Figure 1: Collinear  $\overline{D6} - D6 - \overline{D6}$ .

action is given by

$$S = \int d^5x \left[ -\frac{1}{4g_5^2} F_{MN}^2 + \delta^3(\vec{x}) q_1^\dagger (i\partial_+ + A_+) q_1 + \delta^3(\vec{x} - L_1 \hat{x}_4) q_1^\dagger (i\partial_- + A_-) q_1 + \delta^3(\vec{x} + L_2 \hat{x}_4) q_{\bar{1}}^\dagger (i\partial_- + A_-) q_{\bar{1}} + \delta^3(\vec{x} + L_2 \hat{x}_4) q_{\bar{2}}^\dagger (i\partial_- + A_-) q_{\bar{2}} \right], \quad (2)$$

where  $q_1$  is the left-handed fermion localized at stack 1, and  $q_{\bar{1}}$  and  $q_{\bar{2}}$  are the right-handed fermions localized at stacks  $\bar{1}$  and  $\bar{2}$  respectively. Also  $F_{MN}$ ,  $M, N = 0, 1, 2, 3, 4$ , is the field strength for the five dimensional gauge field  $A_M$ , and  $A_\pm = A_0 \pm A_1$  are its light-cone components.

To leading order in  $\lambda/L_i$ , the dynamics of the fermions can be studied by integrating out the five dimensional gauge field in the single gluon exchange approximation [16]. This can be easily done in Feynman gauge, and one obtains an action with a four-fermion interaction

$$S = \int d^2x \left[ q_1^\dagger i\partial_+ q_1 + q_{\bar{1}}^\dagger i\partial_- q_{\bar{1}} + q_{\bar{2}}^\dagger i\partial_- q_{\bar{2}} \right] + \frac{g_5^2}{4\pi^2} \int d^2x d^2y \left[ G(x - y, L_1) (q_1^\dagger(x) \cdot q_{\bar{1}}(y)) (q_{\bar{1}}^\dagger(y) \cdot q_1(x)) + G(x - y, L_2) (q_1^\dagger(x) \cdot q_{\bar{2}}(y)) (q_{\bar{2}}^\dagger(y) \cdot q_1(x)) \right], \quad (3)$$

where  $G(x, L)$  is the Euclidean propagator

$$G(x, L) = \frac{1}{(x^2 + L^2)^{3/2}}. \quad (4)$$

In the four-fermion interactions, the dot represents color index contractions, while the flavor indices are contracted in the obvious way. This action is a generalization of the non-local

GN model. Now we can further consider the local limit of this model where the fields do not fluctuate over distances of order  $L_i$ , and we consider the theory at distance scales much larger than  $L_i$ <sup>8</sup>. In this limit the propagator essentially behaves as a delta function smeared over distances  $L_i$ , and using

$$\int d^2x G(x, L) = \frac{2\pi}{L} \quad (5)$$

in (3), we get a generalized local GN model with action

$$\begin{aligned} S = & \int d^2x \left[ q_1^\dagger i\partial_+ q_1 + q_{\bar{1}}^\dagger i\partial_- q_{\bar{1}} + q_2^\dagger i\partial_- q_{\bar{2}} \right] \\ & + \frac{1}{N_c} \int d^2x \left[ \frac{2\pi\lambda}{L_1} (q_1^\dagger \cdot q_{\bar{1}}) (q_{\bar{1}}^\dagger \cdot q_1) + \frac{2\pi\lambda}{L_2} (q_1^\dagger \cdot q_{\bar{2}}) (q_{\bar{2}}^\dagger \cdot q_1) \right]. \end{aligned} \quad (6)$$

Note that the couplings of the four-fermion interactions are given by the ratios of the five dimensional 't Hooft coupling and the separations between the branes and the anti-branes.

This model can be exactly solved in the large  $N_c$  limit. We briefly outline the steps involved in analyzing the vacuum structure. We begin by introducing auxiliary bosonic fields and writing the action as

$$\begin{aligned} S = & \int d^2x \left[ q_1^\dagger i\partial_+ q_1 + q_{\bar{1}}^\dagger i\partial_- q_{\bar{1}} + q_2^\dagger i\partial_- q_{\bar{2}} \right] \\ & + \int d^2x \left[ -\frac{1}{N_c} \frac{L_1}{2\pi\lambda} |\phi_1|^2 - \frac{1}{N_c} \frac{L_2}{2\pi\lambda} |\phi_2|^2 + (\bar{\phi}_1 q_1^\dagger \cdot q_{\bar{1}} + \bar{\phi}_2 q_1^\dagger \cdot q_{\bar{2}} + \text{h.c.}) \right]. \end{aligned} \quad (7)$$

In the large  $N_c$  limit, the effective potential can be explicitly evaluated by integrating out the fermions<sup>9</sup>. Using dimensional regularization, we get

$$\frac{V_{\text{eff}}}{N_c} = \frac{L_1}{2\pi\lambda} |\phi_1|^2 + \frac{L_2}{2\pi\lambda} |\phi_2|^2 + \frac{|\phi_1|^2 + |\phi_2|^2}{4\pi} \left[ \ln \left( \frac{|\phi_1|^2 + |\phi_2|^2}{\mu^2} \right) - 1 \right], \quad (8)$$

where  $\mu$  is the renormalization scale.

The effective potential (8) has three extrema

$$\begin{array}{llll} |\phi_1| & |\phi_2| & V_{\text{eff}} & \\ \hline \text{A.} & \mu e^{-L_1/\lambda} & 0 & -\frac{\mu^2 N_c}{4\pi} e^{-2L_1/\lambda} \\ & 0 & \mu e^{-L_2/\lambda} & -\frac{\mu^2 N_c}{4\pi} e^{-2L_2/\lambda} \\ \text{C.} & 0 & 0 & 0 \end{array} \quad (9)$$

<sup>8</sup>As in [16], one can continue to work with the non-local model, however in the limit we work in, it gives the same result.

<sup>9</sup>We quote results for  $N_f = 1$ , these generalize in a straightforward manner for arbitrary  $N_f$ .

While  $C$  is the global maximum, the global minimum is determined by the relative magnitudes of  $L_1$  and  $L_2$ . Without loss of generality, we take  $L_1 < L_2$  for our discussion<sup>10</sup>, and thus the extremum  $A$  corresponds to the vacuum. The field  $\phi_1$  which corresponds to the fermion bilinear  $q_1^\dagger \cdot q_{\bar{1}}$ , acquires a non-vanishing vacuum expectation value, while  $\phi_2$  does not condense. As a result the classical chiral symmetry  $U(N_f)_1 \times U(N_f)_{\bar{1}} \times U(N_f)_{\bar{2}}$  is dynamically broken to  $U(N_f)_{\text{diag}(1, \bar{1})} \times U(N_f)_{\bar{2}}$ . The fermions  $q_1$  and  $q_{\bar{1}}$  acquire mass much smaller than the energy scale  $\mu$  [2], while  $q_{\bar{2}}$  continues to be massless. Note that the extremum  $B$  is tachyonic (along the  $\phi_1$  direction) with mass

$$m^2 = \frac{\partial^2 V_{\text{eff}}}{\partial \phi_1 \partial \bar{\phi}_1} = \frac{2\pi}{\lambda} (L_1 - L_2) < 0. \quad (10)$$

Many of these statements shall have interesting counterparts in the strong coupling regime, which we discuss next.

When  $\lambda/L_i$  is large, the configuration admits a weakly coupled dual description [16] which we briefly review. Consider a stack of D6-branes and a stack of  $\overline{\text{D}6}$ -branes located at  $\pm \frac{L}{2}$  along the 4 direction respectively as shown in figure (2). To study the behavior of

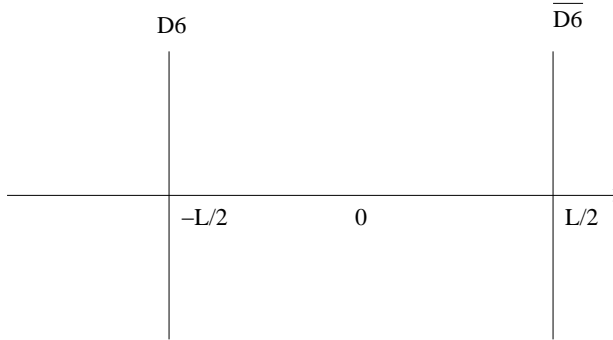


Figure 2: D6- $\overline{\text{D}6}$  pair.

the system at strong coupling, consider a probe D6-brane in the near-horizon geometry of  $N_c$  D4-branes, which is given by the metric and the dilaton

$$\begin{aligned} ds^2 &= \left(\frac{U}{R}\right)^{3/2} [\eta_{\mu\nu} dx^\mu dx^\nu - (dx^4)^2] - \left(\frac{U}{R}\right)^{-3/2} (dU^2 + U^2 d\Omega_4^2), \\ e^\Phi &= g_s \left(\frac{U}{R}\right)^{3/4}, \end{aligned}$$

---

<sup>10</sup>We shall treat the case  $L_1 = L_2$  separately.

where

$$R^3 = \pi\lambda, \quad (11)$$

$U$  is the radial coordinate, and  $\Omega_4$  labels the angular directions in (56789). The analysis in [16] revealed a solution where the D6-brane extends in the (01) directions, wraps the four sphere labeled by  $\Omega_4$  and has a wormhole like profile  $U(x_4)$  which asymptotes to the

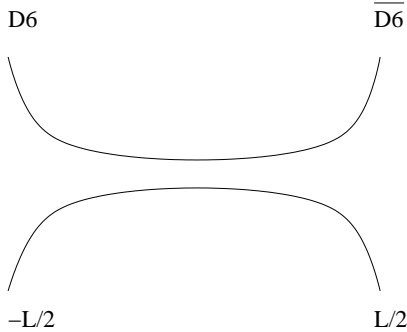


Figure 3: The wormhole.

undeformed D6 and  $\overline{\text{D}6}$ -branes at infinity as shown in figure (3). The wormhole connecting the branes manifestly exhibits chiral symmetry breaking. In fact, one can show that this configuration has less energy than the undeformed D6– $\overline{\text{D}6}$  pair with

$$\delta E(L) \approx -\frac{\lambda^2}{L^4}. \quad (12)$$

Our configuration admits two wormhole solutions, because the D6-branes in stack 1 can connect onto either of the two stacks of  $\overline{\text{D}6}$ -branes at  $\bar{1}$  and  $\bar{2}$  (see figures (4) and (5)).

From (12) we see that energetics requires that the D6-branes in stack 1 connect to the closer  $\overline{\text{D}6}$ -brane stack at  $\bar{1}$ , while  $\bar{2}$  remains disconnected, as depicted in figure (4). Thus as in the weak coupling regime, the classical chiral symmetry  $U(N_f)_1 \times U(N_f)_{\bar{1}} \times U(N_f)_{\bar{2}}$  is broken to  $U(N_f)_{\text{diag}(1,\bar{1})} \times U(N_f)_{\bar{2}}$ .

Note that the strong coupling counterpart of vanishing  $\phi_2$  condensate is the absence of a wormhole connecting stacks 1 and  $\bar{2}$ . This illustrates an interesting point about general D-brane configurations at strong coupling. At strong coupling, all “condensates” except those corresponding to the pairs of branes and anti-branes which are connected by wormholes vanish. In all examples we will consider later in the paper, we find that the weak coupling vacuum structure has behavior which seems to be reminiscent of this property.

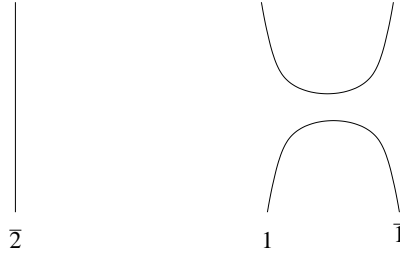


Figure 4: Vacuum configuration.

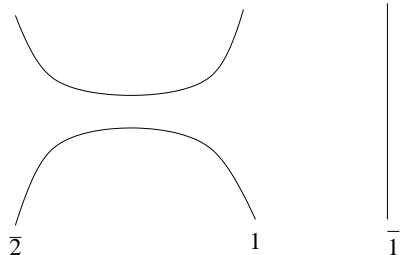


Figure 5: Metastable configuration.

The energetically disfavored configuration in figure (5) has the same symmetries as the extremum B in (9) and it is natural to think of it as the strong coupling continuation of B. We note that the corresponding wormhole configuration is metastable, while B in (9) has a tachyon given by (10) .

Finally, we consider the particular case when  $L_1 = L_2 \equiv L$ . In the weak coupling regime, from (3) we see that the non-local GN model (and consequently the local GN model) has an enhanced  $U(N_f)_L \times U(2N_f)_R$  chiral symmetry under which

$$\begin{pmatrix} q_{\bar{1}} \\ q_{\bar{2}} \end{pmatrix}$$

transforms in the  $2N_f$  dimensional representation of  $U(2N_f)_R$ . Thus

$$\begin{pmatrix} \phi_1 \\ \phi_2 \end{pmatrix}$$

also transforms in the same way. In this case, the vacuum configuration of the GN model is given by

$$|\phi_1|^2 + |\phi_2|^2 = \mu^2 e^{-2L/\lambda}, \quad (13)$$

which leads to the vacuum energy

$$V_{\text{eff}} = -\frac{\mu^2 N_c}{4\pi} e^{-2L/\lambda}. \quad (14)$$

Thus the  $U(N_f)_L \times U(2N_f)_R$  chiral symmetry is dynamically broken to  $U(N_f)_{\text{diag}(L,R)} \times U(N_f)_R$ . At strong coupling, this symmetry breaking manifests itself in the fact that the wormhole can connect the D6-brane with either of the two  $\overline{\text{D}6}$ -branes as they both have the same energy.

### 3.2 $\text{D}6 - \overline{\text{D}6} - \overline{\text{D}6}$

The other configuration involves placing the branes and anti-branes in the order  $\text{D}6 - \overline{\text{D}6} - \overline{\text{D}6}$  as shown in figure (6).

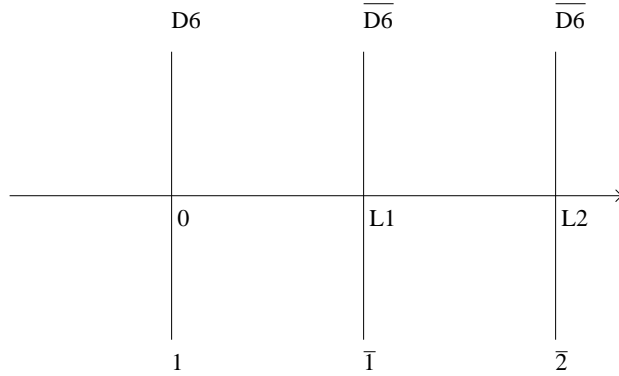


Figure 6: Collinear  $\text{D}6 - \overline{\text{D}6} - \overline{\text{D}6}$ .

We place the stack of D6-branes at the origin and the two stacks of  $\overline{\text{D}6}$ -branes at  $L_1$  and  $L_2$ , where  $L_2 > L_1$ . The analysis can be easily carried out making use of the results of the previous section. At weak coupling, the couplings between the left and right-handed fermions depend only of the distances between the brane and anti-brane pairs. Hence the vacuum energy density is identical to the previous case and is given by (8). From (9) we see that  $\phi_1$  has a non-vanishing vacuum expectation value, and so the classical  $U(N_f)_1 \times U(N_f)_{\bar{1}} \times U(N_f)_{\bar{2}}$  chiral symmetry is dynamically broken to  $U(N_f)_{\text{diag}(1, \bar{1})} \times U(N_f)_{\bar{2}}$ .

At strong coupling, the D6-brane is connected to the anti  $\overline{D6}$ -brane closer to it through a wormhole as shown in figure (7).

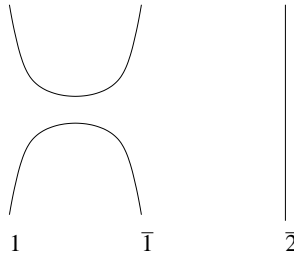


Figure 7:  $U(N_f)_1 \times U(N_f)_{\bar{1}} \times U(N_f)_{\bar{2}} \rightarrow U(N_f)_{\text{diag}(1, \bar{1})} \times U(N_f)_{\bar{2}}$ .

## 4 More patterns of chiral symmetry breaking

Having analyzed chiral symmetry breaking in three collinear stacks of flavor branes, we now consider more general patterns involving D-brane configurations which have equal numbers of D6 and  $\overline{D6}$ -branes. First, we shall consider four collinear stacks of flavor branes. Then we shall consider two simple D-brane configurations spanning an  $\mathbb{R}^2$  in  $\mathbb{R}^3$ . Apart from being useful models to study patterns of chiral symmetry breaking, these constructions will be helpful in analyzing the general pattern of symmetry breaking involving arbitrary configurations of flavor branes in  $\mathbb{R}^3$ . As before we find that the patterns of chiral symmetry breaking are similar at weak and strong coupling.

### 4.1 Four collinear flavor branes

In this section we shall consider configurations with two stacks of D6-branes, and two stacks of  $\overline{D6}$ -branes placed along the 4 direction. We shall label the D6-brane stacks by indices 1, 2, and denote their coordinates by  $L_1, L_2$  respectively. Similarly, we denote the  $\overline{D6}$ -brane stacks by  $\bar{1}, \bar{2}$ , and denote their coordinates by  $L_{\bar{1}}, L_{\bar{2}}$  respectively. We also use  $L_{i\bar{j}}$  to denote the distance between the  $i$ -th D6-brane and the  $\bar{j}$ -th  $\overline{D6}$ -brane.

We first consider the weak coupling limit and obtain the effective potential. As in the three stack case, to leading order in  $\lambda/L_{i\bar{j}}$ , the dynamics of the fermions at length scales much greater than the D-brane separations can be described by a local GN model

obtained by integrating out the five dimensional gauge field in the single gluon exchange approximation. Once again, the effective field theory is a generalized GN model with two left-moving and two right-moving fermions, and is given by

$$S = \int d^2x \left[ \sum_i q_i^\dagger i\partial_+ q_i + \sum_{\bar{j}} q_{\bar{j}}^\dagger i\partial_- q_{\bar{j}} + \frac{1}{N_c} \sum_{i,\bar{j}} \frac{2\pi\lambda}{L_{i\bar{j}}} (q_i^\dagger \cdot q_{\bar{j}}) (q_{\bar{j}}^\dagger \cdot q_i) \right]. \quad (15)$$

After introducing auxiliary fields  $\phi_{i\bar{j}}$  corresponding to fermion bilinears  $q_i^\dagger \cdot q_{\bar{j}}$  and integrating out the fermions, one obtains the effective potential in the large  $N_c$  limit

$$\frac{V_{\text{eff}}}{N_c} = \sum_{i,\bar{j}} \frac{L_{i\bar{j}}}{2\pi\lambda} |\phi_{i\bar{j}}|^2 + \frac{\theta + \sqrt{\delta}}{8\pi} \left[ \ln\left(\frac{\theta + \sqrt{\delta}}{2\mu^2}\right) - 1 \right] + \frac{\theta - \sqrt{\delta}}{8\pi} \left[ \ln\left(\frac{\theta - \sqrt{\delta}}{2\mu^2}\right) - 1 \right], \quad (16)$$

where

$$\theta = \sum_{i,\bar{j}} |\phi_{i\bar{j}}|^2, \quad \delta = \left( \sum_{i,\bar{j}} |\phi_{i\bar{j}}|^2 \right)^2 - 4|\phi_{1\bar{1}}\phi_{2\bar{2}} - \phi_{1\bar{2}}\phi_{2\bar{1}}|^2. \quad (17)$$

The properties of the vacuum configuration obtained by minimizing (16) are closely related to the ordering of the stacks (i.e., the relative magnitudes of  $L_{i\bar{j}}$ ). Up to charge conjugation, there are three distinct orderings D6 – D6 –  $\overline{\text{D6}}$  –  $\overline{\text{D6}}$ , D6 –  $\overline{\text{D6}}$  –  $\overline{\text{D6}}$  – D6 and D6 –  $\overline{\text{D6}}$  – D6 –  $\overline{\text{D6}}$ . We discuss each case separately, also illustrating the relationship to wormhole solutions at strong coupling.

#### 4.1.1 D6 – D6 – $\overline{\text{D6}}$ – $\overline{\text{D6}}$

For this ordering given by figure (8), the minimum of the effective potential (16) is given by

$$|\phi_{1\bar{2}}| = \mu e^{-L_{1\bar{2}}/\lambda}, \quad |\phi_{2\bar{1}}| = \mu e^{-L_{2\bar{1}}/\lambda}, \quad \phi_{1\bar{1}} = 0, \quad \phi_{2\bar{2}} = 0. \quad (18)$$

Thus the classical  $U(N_f)_1 \times U(N_f)_2 \times U(N_f)_{\bar{1}} \times U(N_f)_{\bar{2}}$  chiral symmetry is broken to  $U(N_f)_{\text{diag}(1,\bar{2})} \times U(N_f)_{\text{diag}(2,\bar{1})}$ . At strong coupling the wormhole configuration with the lowest energy is shown in figure (9), which exhibits the same symmetry breaking pattern<sup>11</sup>.

#### 4.1.2 D6 – $\overline{\text{D6}}$ – $\overline{\text{D6}}$ – D6

In this case given by figure (10), the minimum of the effective potential (16) is given by

$$|\phi_{1\bar{1}}| = \mu e^{-L_{1\bar{1}}/\lambda}, \quad |\phi_{2\bar{2}}| = \mu e^{-L_{2\bar{2}}/\lambda}, \quad \phi_{1\bar{2}} = 0, \quad \phi_{2\bar{1}} = 0, \quad (19)$$

<sup>11</sup>The difference between the radii of the two wormholes at the point of closest approach is much larger than  $\sqrt{\alpha'}$  for sufficiently large values of  $\lambda/L_{i\bar{j}}$ , thus the gravity construction can be trusted.

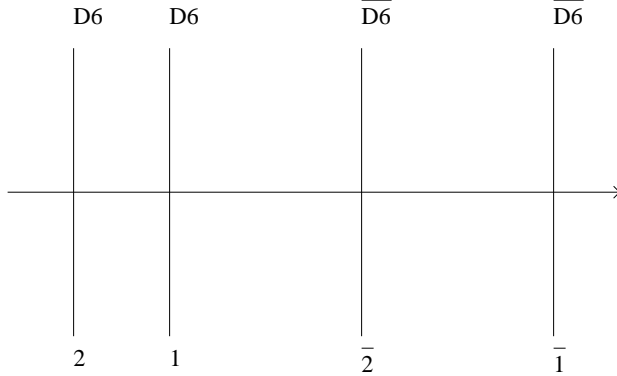


Figure 8: Collinear  $D6 - D6 - \bar{D6} - \bar{D6}$ .

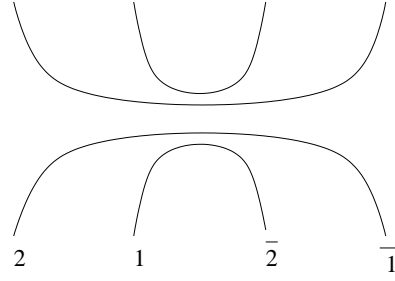


Figure 9:  $U(N_f)_1 \times U(N_f)_2 \times U(N_f)_{\bar{1}} \times U(N_f)_{\bar{2}} \rightarrow U(N_f)_{\text{diag}(1, \bar{2})} \times U(N_f)_{\text{diag}(2, \bar{1})}$ .

and the chiral symmetry is dynamically broken to  $U(N_f)_{\text{diag}(1, \bar{1})} \times U(N_f)_{\text{diag}(2, \bar{2})}$ . Again, the energetically favorable wormhole configuration is shown in figure (11), which exhibits the same symmetry breaking pattern.

#### 4.1.3 $D6 - \bar{D6} - D6 - \bar{D6}$

This case as shown in figure (12) exhibits more interesting structure of chiral symmetry breaking. The nature of the vacuum structure explicitly depends on the separations of the stacks. At weak coupling, simple energetics using the effective potential (16) shows that for

$$e^{-2L_{1\bar{1}}/\lambda} + e^{-2L_{2\bar{2}}/\lambda} > e^{-2L_{1\bar{2}}/\lambda} + e^{-2L_{2\bar{1}}/\lambda}, \quad (20)$$

the vacuum has condensates

$$X : |\phi_{1\bar{1}}| = \mu e^{-L_{1\bar{1}}/\lambda}, \quad |\phi_{2\bar{2}}| = \mu e^{-L_{2\bar{2}}/\lambda}, \quad \phi_{1\bar{2}} = 0, \quad \phi_{2\bar{1}} = 0. \quad (21)$$

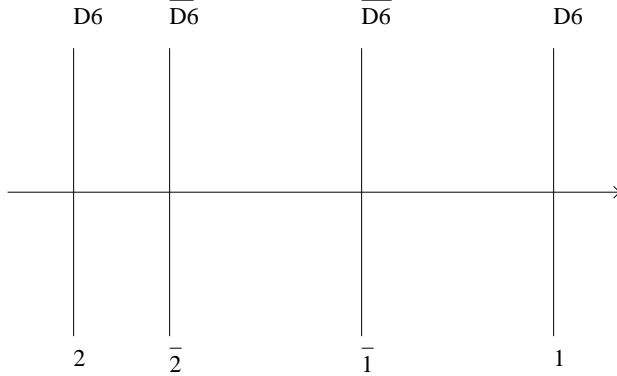


Figure 10: Collinear  $D6 - \overline{D6} - \overline{D6} - D6$ .



Figure 11:  $U(N_f)_1 \times U(N_f)_2 \times U(N_f)_{\bar{1}} \times U(N_f)_{\bar{2}} \rightarrow U(N_f)_{\text{diag}(1, \bar{1})} \times U(N_f)_{\text{diag}(2, \bar{2})}$ .

On the other hand, when the inequality in (20) is reversed the condensates are

$$Y : |\phi_{1\bar{2}}| = \mu e^{-L_{1\bar{2}}/\lambda}, \quad |\phi_{2\bar{1}}| = \mu e^{-L_{2\bar{1}}/\lambda}, \quad \phi_{1\bar{1}} = 0, \quad \phi_{2\bar{2}} = 0. \quad (22)$$

Note that X and Y represent two distinct phases, with different symmetries of the vacuum.

Similarly in the strong coupling regime, there are two patterns of chiral symmetry breaking determined by the energetics of the wormhole configurations. For

$$\frac{1}{L_{1\bar{1}}^4} + \frac{1}{L_{2\bar{2}}^4} > \frac{1}{L_{1\bar{2}}^4} + \frac{1}{L_{2\bar{1}}^4}, \quad (23)$$

the energetically favored configuration is shown in figure (13). On the other hand, the configuration in figure (14) is energetically favored when the inequality in (23) is reversed. The configurations in figures (13) and (14) preserve the same symmetries as the phases X

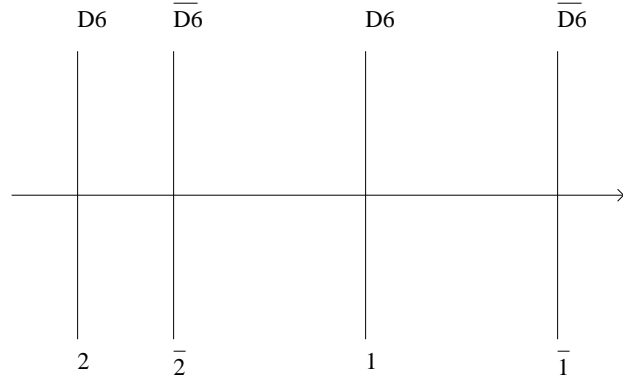


Figure 12: Collinear  $D6 - \overline{D6} - D6 - \overline{D6}$ .

and  $Y$  respectively. They should be thought of as the strong coupling continuations of these phases.



Figure 13:  $U(N_f)_1 \times U(N_f)_2 \times U(N_f)_{\bar{1}} \times U(N_f)_{\bar{2}} \rightarrow U(N_f)_{\text{diag}(1, \bar{1})} \times U(N_f)_{\text{diag}(2, \bar{2})}$ .

From the structure of the inequalities (20) and (23), we expect that at an arbitrary coupling the vacuum is in a phase determined by an inequality of the form

$$f\left(\frac{\lambda}{L_{1\bar{1}}}\right) + f\left(\frac{\lambda}{L_{2\bar{2}}}\right) > f\left(\frac{\lambda}{L_{1\bar{2}}}\right) + f\left(\frac{\lambda}{L_{2\bar{1}}}\right), \quad (24)$$

where  $f(x)$  is a monotonically increasing function of  $x$ , and

$$f(x) \rightarrow \begin{cases} e^{-2/x}, & \text{as } x \rightarrow 0, \\ x^4, & \text{as } x \rightarrow \infty. \end{cases}$$

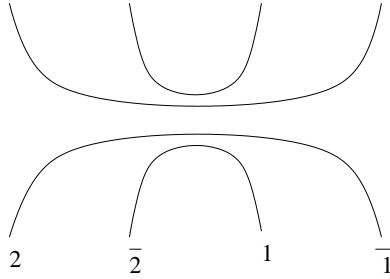


Figure 14:  $U(N_f)_1 \times U(N_f)_2 \times U(N_f)_{\bar{1}} \times U(N_f)_{\bar{2}} \rightarrow U(N_f)_{\text{diag}(1, \bar{2})} \times U(N_f)_{\text{diag}(2, \bar{1})}$ .

## 4.2 Four flavor branes spanning two dimensions

So far we have considered stacks of flavor branes that lie along a straight line in  $\mathbb{R}^3$ . In order to understand the general patterns of chiral symmetry breaking, it is useful to look at flavor brane configurations that are not collinear. With this in mind, we analyze chiral symmetry breaking in the two simplest D-brane configurations spanning an  $\mathbb{R}^2$  in  $\mathbb{R}^3$ , both at weak and strong coupling. These two configurations are given by two stacks of D6-branes and two stacks of  $\overline{\text{D}6}$ -branes lying in a plane in  $\mathbb{R}^3$ , such that they form a rectangle. There are two distinct orderings of the D-branes (upto charge conjugation), as we discuss below.

### 4.2.1 $\text{D}6 - \overline{\text{D}6} - \overline{\text{D}6} - \overline{\text{D}6}$ rectangle

We consider the D6 and  $\overline{\text{D}6}$ -branes as depicted in figure (15) forming a rectangle in  $\mathbb{R}^2$ . In the diagram, each stack of D6 ( $\overline{\text{D}6}$ )-branes is represented by a point, given by a vertex of the rectangle.

Proceeding as before, at weak coupling, the non-vanishing condensates are given by

$$|\phi_{1\bar{2}}| = \mu e^{-L_{1\bar{2}}/\lambda} = \mu e^{-L_{2\bar{1}}/\lambda} = |\phi_{2\bar{1}}|, \quad \phi_{1\bar{1}} = 0, \quad \phi_{2\bar{2}} = 0. \quad (25)$$

Similarly in the strong coupling limit, there are two wormholes connecting the corresponding vertices of the rectangle.

### 4.2.2 $\text{D}6 - \overline{\text{D}6} - \text{D}6 - \overline{\text{D}6}$ rectangle

Finally, we consider the other possible configuration of D6 and  $\overline{\text{D}6}$ -branes which form a rectangle in  $\mathbb{R}^2$  as depicted in figure (16). At weak coupling, if  $L_{1\bar{1}} > L_{1\bar{2}}$ , the non-vanishing

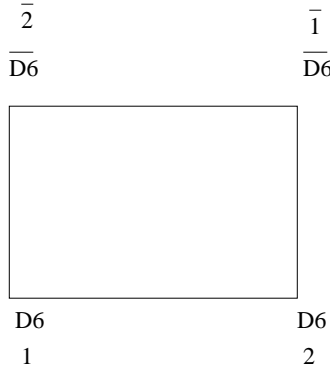


Figure 15:  $D6 - D6 - \overline{D6} - \overline{D6}$  rectangle.

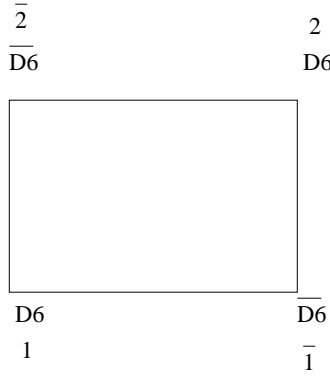


Figure 16:  $D6 - \overline{D6} - D6 - \overline{D6}$  rectangle.

condensates are given by

$$|\phi_{1\bar{2}}| = \mu e^{-L_{1\bar{2}}/\lambda} = \mu e^{-L_{2\bar{1}}/\lambda} = |\phi_{2\bar{1}}|, \quad \phi_{1\bar{1}} = 0, \quad \phi_{2\bar{2}} = 0. \quad (26)$$

On the other hand, if  $L_{1\bar{2}} > L_{1\bar{1}}$ , the non-vanishing condensates are given by

$$|\phi_{1\bar{1}}| = \mu e^{-L_{1\bar{1}}/\lambda} = \mu e^{-L_{2\bar{2}}/\lambda} = |\phi_{2\bar{2}}|, \quad \phi_{1\bar{2}} = 0, \quad \phi_{2\bar{1}} = 0. \quad (27)$$

At strong coupling, there are corresponding wormhole solutions along the corresponding edges of the rectangle in an obvious way.

Now when  $L_{1\bar{1}} = L_{1\bar{2}}$ , the D-brane configuration has an enhanced  $U(2N_f)_L \times U(2N_f)_R$  chiral symmetry classically, which gets dynamically broken to  $U(N_f)_{\text{diag(L,R)}} \times U(N_f)_{\text{diag(L,R)}}$  both at weak and strong coupling.

## 5 General patterns of chiral symmetry breaking and restoration at high temperature

From the above examples, one can see the general patterns of chiral symmetry breaking both at weak coupling as well as at strong coupling. In the weak coupling limit, in the single gluon exchange approximation, we always get a generalized non-local GN model. Furthermore restricting to length scales much larger than the separations between the flavor branes, we end up getting local GN models. Interactions in these models depend only on the distances  $L_{i\bar{j}}$  between a stack of D6-branes and another stack of  $\overline{\text{D}6}$ -branes placed at  $L_i$  and  $L_{\bar{j}}$  respectively, through the corresponding GN coupling  $\lambda/L_{i\bar{j}}$ . In particular, the coupling between a D6– $\overline{\text{D}6}$  pair does not depend on the angular orientation of the two stacks in  $\mathbb{R}^3$ . Thus in general, we will have generalized GN models with all possible couplings, and the vacuum configuration will be determined by the energetics; namely, the vacuum configuration will have non-vanishing condensates of only those fermion bilinears connecting the D6– $\overline{\text{D}6}$  pairs such that the energy is at its global minimum. On the basis of the constructions we have described, we expect that in any D-brane configuration with equal number of stacks of D6 and  $\overline{\text{D}6}$ -branes, the vacuum configuration will always have non-vanishing condensates such that all the fermions get mass dynamically. We also expect that if there are  $P$  stacks of D6-branes and  $Q$  stacks of  $\overline{\text{D}6}$ -branes such that  $P \neq Q$ , the vacuum configuration will have  $|P - Q|$  stacks of unpaired D6 ( $\overline{\text{D}6}$ ) branes, depending on whether  $P > Q$  ( $P < Q$ ). For certain D-brane configurations, there can be enhanced chiral symmetries. For example, if a stack of D6-branes is equidistant from  $K$  stacks of  $\overline{\text{D}6}$ -branes in  $\mathbb{R}^3$ , then the configuration has an enhanced  $U(N_f)_L \times U(KN_f)_R$  chiral symmetry, which is dynamically broken to  $U(N_f)_{\text{diag}(L,R)} \times U((K-1)N_f)_R$ . At weak coupling, one has a condensate given by a fermion bilinear involving the left-moving fermions from the D6-brane stack and the right-moving fermions from any one of the  $K$   $\overline{\text{D}6}$ -brane stacks. In the strong coupling limit, the analogues of condensates are wormholes. The vacuum configuration is determined by the the energetics of wormholes connecting pairs of D6-branes and  $\overline{\text{D}6}$ -branes.

We have so far analyzed the chiral symmetry breaking which occurs at infinite  $N_c$  at zero temperature. If we now start heating the system to higher and higher temperatures, the chiral symmetry gets restored as we now explain. In the GN model, it is well known that the chiral symmetry is restored at a temperature  $T_c$  given by [19–21]

$$T_c = 0.57m_f, \quad (28)$$

where  $m_f$  is the dynamically generated mass for the fermions at zero temperature. In fact, this phase transition is second order in nature. Thus in the weak coupling limit where we obtain the generalized GN models, there is chiral symmetry restoration at temperatures given by

$$T_c(L_{i\bar{j}}) = 0.57\mu e^{-L_{i\bar{j}}/\lambda(\mu)}. \quad (29)$$

So as we heat up the system from zero temperature, the condensates start evaporating as soon as the corresponding phase transition temperatures are attained. Thus at a sufficiently high temperature, all the symmetries are restored. The strong coupling analysis is similar, with the phase transition temperature given by [16]<sup>12</sup>

$$T_c(L_{i\bar{j}}) \approx \frac{0.205}{L_{i\bar{j}}}. \quad (30)$$

However, now the phase transition is first order in nature.

Thus we see that the D-brane configurations we have discussed above exhibit interesting patterns of chiral symmetry breaking. The construction of generalized GN models from string theory opens up several directions which might be worth looking at. It would be nice to understand the spectrum of bound states, solitons and their interactions in these theories both at weak and strong coupling, and possibly also at finite values of the coupling. Also one might be interested in analyzing the integrability of these theories to compute the S-matrix. It might also be useful to analyze configurations where there are directions transverse to both the color and the flavor branes, which enable us to give tunable masses to the fermions. These techniques are generalizable to other D-brane configurations and might be useful in understanding generalized models of chiral symmetry breaking in other dimensions, thus generalizing the results in [24]. Finally, one can also analyze generalized models of QCD<sub>2</sub> by wrapping the D4-branes on  $T^3$  [16]<sup>13</sup> as mentioned before.

## Acknowledgements

We would like to thank S. Giddings, J. Maldacena, P. Ouyang, and J. Polchinski for useful discussions. The work of A. B. and A. M. is supported by NSF Grant No. PHY-0503584, and DOE Grant No. DE-FG02-91ER40618 respectively.

---

<sup>12</sup>This has been analyzed for the  $D4 - D8 - \overline{D8}$  case in [22, 23].

<sup>13</sup>A construction of QCD<sub>2</sub> using a different D-brane configuration has been done in [25].

## References

- [1] Y. Nambu and G. Jona-Lasinio, “Dynamical model of elementary particles based on an analogy with superconductivity. I,” *Phys. Rev.* **122** (1961) 345–358.
- [2] D. J. Gross and A. Neveu, “Dynamical symmetry breaking in asymptotically free field theories,” *Phys. Rev.* **D10** (1974) 3235.
- [3] S. R. Coleman and E. Weinberg, “Radiative corrections as the origin of spontaneous symmetry breaking,” *Phys. Rev.* **D7** (1973) 1888–1910.
- [4] E. Witten, “Chiral symmetry, the  $1/N$  expansion, and the  $SU(N)$  Thirring model,” *Nucl. Phys.* **B145** (1978) 110.
- [5] I. Affleck, “On the realization of chiral symmetry in (1+1)-dimensions,” *Nucl. Phys.* **B265** (1986) 448.
- [6] E. Witten, “Anti-de Sitter space, thermal phase transition, and confinement in gauge theories,” *Adv. Theor. Math. Phys.* **2** (1998) 505–532, [hep-th/9803131](#).
- [7] T. Sakai and S. Sugimoto, “Low energy hadron physics in holographic QCD,” *Prog. Theor. Phys.* **113** (2005) 843–882, [hep-th/0412141](#).
- [8] T. Sakai and S. Sugimoto, “More on a holographic dual of QCD,” *Prog. Theor. Phys.* **114** (2006) 1083–1118, [hep-th/0507073](#).
- [9] A. Karch and E. Katz, “Adding flavor to AdS/CFT,” *JHEP* **06** (2002) 043, [hep-th/0205236](#).
- [10] D. T. Son and M. A. Stephanov, “QCD and dimensional deconstruction,” *Phys. Rev.* **D69** (2004) 065020, [hep-ph/0304182](#).
- [11] M. Kruczenski, D. Mateos, R. C. Myers, and D. J. Winters, “Towards a holographic dual of large- $N(c)$  QCD,” *JHEP* **05** (2004) 041, [hep-th/0311270](#).
- [12] J. Babington, J. Erdmenger, N. J. Evans, Z. Guralnik, and I. Kirsch, “Chiral symmetry breaking and pions in non-supersymmetric gauge / gravity duals,” *Phys. Rev.* **D69** (2004) 066007, [hep-th/0306018](#).
- [13] E. Antónyan, J. A. Harvey, S. Jensen, and D. Kutasov, “NJL and QCD from string theory,” [hep-th/0604017](#).

- [14] D. Bak and H.-U. Yee, “Separation of spontaneous chiral symmetry breaking and confinement via AdS/CFT correspondence,” *Phys. Rev.* **D71** (2005) 046003, [hep-th/0412170](#).
- [15] M. K. Volkov and A. E. Radzhabov, “Forty-fifth anniversary of the Nambu-Jona-Lasinio model,” [hep-ph/0508263](#).
- [16] E. Antonyan, J. A. Harvey, and D. Kutasov, “The Gross-Neveu model from string theory,” [hep-th/0608149](#).
- [17] K. G. Klimenko, “Generalization of Gross-Neveu model to the case of several coupling constants,” *Theor. Math. Phys.* **66** (1986) 252.
- [18] N. Itzhaki, J. M. Maldacena, J. Sonnenschein, and S. Yankielowicz, “Supergravity and the large N limit of theories with sixteen supercharges,” *Phys. Rev.* **D58** (1998) 046004, [hep-th/9802042](#).
- [19] L. Jacobs, “Critical behavior in a class of  $O(N)$  invariant field theories in two-dimensions,” *Phys. Rev.* **D10** (1974) 3956.
- [20] B. J. Harrington and A. Yildiz, “Restoration of dynamically broken symmetries at finite temperature,” *Phys. Rev.* **D11** (1975) 779.
- [21] R. F. Dashen, S.-k. Ma, and R. Rajaraman, “Finite temperature behavior of a relativistic field theory with dynamical symmetry breaking,” *Phys. Rev.* **D11** (1975) 1499.
- [22] O. Aharony, J. Sonnenschein, and S. Yankielowicz, “A holographic model of deconfinement and chiral symmetry restoration,” [hep-th/0604161](#).
- [23] A. Parnachev and D. A. Sahakyan, “Chiral phase transition from string theory,” [hep-th/0604173](#).
- [24] E. Antonyan, J. A. Harvey, and D. Kutasov, “Chiral symmetry breaking from intersecting D-branes,” [hep-th/0608177](#).
- [25] Y.-h. Gao, W.-s. Xu, and D.-f. Zeng, “NGN, QCD(2) and chiral phase transition from string theory,” *JHEP* **08** (2006) 018, [hep-th/0605138](#).